Reports

Galilean Satellites: Identification of Water Frost

Abstract. *Water frost absorptions have been detected in the infrared reflectivities of Jupiter's Galilean satellites JII (Europa) and JIII (Ganymede). We have determined the percentage of frost-covered surface area to be 50 to 100 percent for JII, 20 to 65 percent for JIII, and possibly 5 to 25 percent for JIV (Callisto). The leading side of JIII has 20 percent more frost cover than the trailing side, which explains the visible geometric albedo differences between the two sides. The reflectivity of the material underlying the frost on JII, JIII, and JIV resembles that of silicates. The surface of JI (Io) may be covered by frost particles much smaller than those on JII and JIII.*

We have conclusively identified absorptions due to water frost in the infrared reflectivities of Jupiter's Galilean satellites JII and JIII. Water frost (or ice) has long been thought to be a constituent of these and other bodies in the outer solar system. Kuiper (*1*) suggested the presence of water ice in the rings and the six inner satellites of Saturn, satellites JIII and JIV of Jupiter, Triton, and Pluto. McCord *et al.* (*2*) showed that the reflectivities (from 0.3 to 1.1 μm) of four satellites of Saturn are consistent with ice surfaces. Pilcher *et al.* (*3*) first identified water frost in the infrared spectrum of Saturn's rings (*4*). Kuiper (*5*) and Moroz (*6*) showed that JII and JIII have lower reflectivities at 2 μm than at 1 μm, as do many ices (*7, 8*). Gromova *et al.* (*9*) and Johnson and McCord (*10*) measured a depression in the reflectivity of JII and JIII near 1.6 μm (6250 cm^{-1}), suggestive of water or ammonia frost (*3*). Morrison and Cruikshank (*11*) found that variations in the intensity of emitted thermal infrared radiation during eclipses of JI, JIII, and JIV are consistent with a thin surface layer of frost covering a denser mixture of rock and ice. Lewis (*12*) suggested, on theoretical grounds, the presence of nearly pure water ice crusts on the Galilean satellites (JI through JIV).

We have measured the reflectivities of the Galilean satellites from 2500 to 8000 cm^{-1} (1.25 to 4.0 μm) at a resolution of 33 cm^{-1} (66 Å at 2.0 μm) by using a rapid scanning Fourier spectrometer on the 60-inch (152.4-cm) McMath solar telescope of Kitt Peak National Observatory (Table 1). For comparison with laboratory data, the reflectivities have been smoothed to a resolution of 120 cm^{-1}, reducing the effective observing times to those given in Table 1. No features narrower than 120 cm^{-1} were present in the original reflectivities.

Each observation was reduced by the methods of Johnson *et al.* (*13*) by using observations at equal air mass to form a ratio of the intensity of the satellite spectrum ($I_{\rm sat}$) to that of the spectrum of the star λSgr ($I_{\lambda{\rm Sgr}}$). Similarly, a ratio was formed of the intensity of the λSgr spectrum to that of the spectrum of the lunar crater Fra Mauro ($I_{\rm moon}$). The satellite reflectivity is given by

$$R_{\rm sat} = \left[\frac{I_{\rm sat}}{I_{\lambda{\rm Sgr}}}\right]\left[\frac{I_{\lambda{\rm Sgr}}}{I_{\rm moon}}\right]R^{\rm ref}_{\rm moon} = \left[\frac{R_{\rm sat}\,I_{\odot}}{I_{\lambda{\rm Sgr}}}\right]\left[\frac{I_{\lambda{\rm Sgr}}}{(R_{\rm moon})\,(I_{\odot})}\right]R^{\rm ref}_{\rm moon} \qquad (1)$$

where $I_{\odot}$ is the solar intensity. The reference lunar reflectivity ($R^{\rm ref}_{\rm moon}$) was that of a small area in Mare Serenitatis given by McCord and Johnson (*14*) from 0.3 to 2.5 μm (4000 to 33,000 cm^{-1}) and extrapolated by us to 4.0 μm (2500 cm^{-1}). For our purposes, the reflectivity of this area is sufficiently similar to those of upland areas such as the Fra Mauro region (*14*). The reflectivities of JI and JIV, the only satellites from which we detected radiation between 2500 and 3300 cm^{-1} (3 and 4 μm), are not corrected for lunar emission in that region and are therefore reduced below their proper values.

The satellite reflectivities are presented in Fig. 1. Each accompanying error bar represents the average of the standard deviations for all wavelengths. The curves are broken where there was no measurable signal because of atmospheric absorption. The reflectivities in Fig. 1 refer to one side of each satellite, if synchronous rotation is assumed (*15, 16*). The terms "leading side" and "trailing side" refer, respectively, to the sides of the satellite facing toward and away from its direction of motion about Jupiter. The reflectivities have been scaled approximately to the geometric albedos of Johnson and McCord (*10*); their JI albedos were corrected by using the stellar occultation radius of JI (*17*). Our signal-to-noise ratio is much higher than theirs, in part because of the interferometric multiplex advantage described by Fellgett (*18*).

Absorptions due to water frost, as measured in the laboratory by Kieffer (*8*) and presented in Fig. 1, can be readily identified in the reflectivities of JII and JIII. They appear as minima at 6700, 6450 (a shoulder in the JII reflectivity), 6100, and 5000 cm^{-1} (1.49, 1.55, 1.64, and 2.0 μm, respectively). The relative intensities of these absorptions are dependent on the temperature history (*8, 19*) and particle size (*7*) of the frost in ways compatible with the minor differences between the satellite and laboratory frost data. The noisy reflectivity of JIV shows broad, weak absorptions near 6600 and 4950 cm^{-1} (1.52 and 2.05 μm), consistent with some water frost on JIV. The JI reflectivity also shows a broad weak absorption near 6600 cm^{-1} and a possible absorption near 4950 cm^{-1}, as well as many narrow noise features. Our detection of radiation only from JI and JIV between 2500 and 3300 cm^{-1} is consistent with the results of Gillett *et al.* (*20*).

The water frost absorptions are strongest for JII, weaker for JIII, and, if present, extremely weak for JI and JIV. This decrease in absorption intensities for JII through JIV may be due to a similar decrease in the frost-covered fraction of each satellite's surface. If so, the fraction for each satellite can be estimated. The depth of the absorption at 5000 cm^{-1} for JII implies that no less than 75 percent of the observed infrared radiation is reflected by water frost. Assuming values of 0.5 for the geometric albedo of water frost (*7, 8*) and 0.35 (typical of silicates) for the geometric albedo of the underlying material (*21*), we find that about 70 percent of the surface of JII is frost covered.

Using other reasonable values for the geometric albedos, we conclude that the limits for frost cover on the leading side of JII are 50 to 100 percent of its surface area. From the weaker absorptions in the JIII reflectivity, we find that about 50 percent of the observed radiation is reflected by water frost. By the same reasoning as in the case of JII, the limits for frost cover on the leading side of JIII are 20 to 65 percent of its surface area. The reflectivity of JIV is consistent with approximately 15 percent of the observed radiation being reflected by water frost; this yields a surface frost cover of 5 to 5 percent.

Table 1. Information on the observations. The abbreviations are: L, leading side; T, trailing side; N, number of independent measurements; t_{eff}, effective observing time. In calculating t_{eff} allowance was made for smoothing the data.

Satellite	Side	Date observed (1972)	N	t_{eff} (min)
JI	L	30 June, 2 July	2	25
JII	L	27 June	6	75
JIII	L	26 June	5	62
JIII	T	30 June	5	62
JIV	T	30 June, 2 July	4	50

The visible geometric albedos of the satellites measured by Johnson (*22*) are consistent with this variable frost cover model. At 0.56 μm the geometric albedos are 0.68 (JI), 0.80 (JII), 0.62 (JIII), and 0.27 (JIV). The albedo of JI has been corrected by using the stellar occultation value for the radius of JI. Assuming the visible geometric albedos of water frost and the underlying material (for example, silicates) to be 0.8 and 0.15, respectively, and the fractional frost covers of JII through JIV to be 0.7, 0.4, and 0.1, respectively, we obtain the following values for the ratios of the visible geometric albedos: JII/JIII = 1.5 and JII/JIV = 2.8. These compare favorably with the observed values of 1.3 and 3.0. Exact agreement is obtained with fractional frost covers of 0.7, 0.5, and 0.08 for JII, JIII, and JIV, respectively.

Decreasing absorption intensities in frost spectra can also be produced by decreasing the size of the frost particles (*7*). But as the particle size of a frost decreases its visible albedo increases,

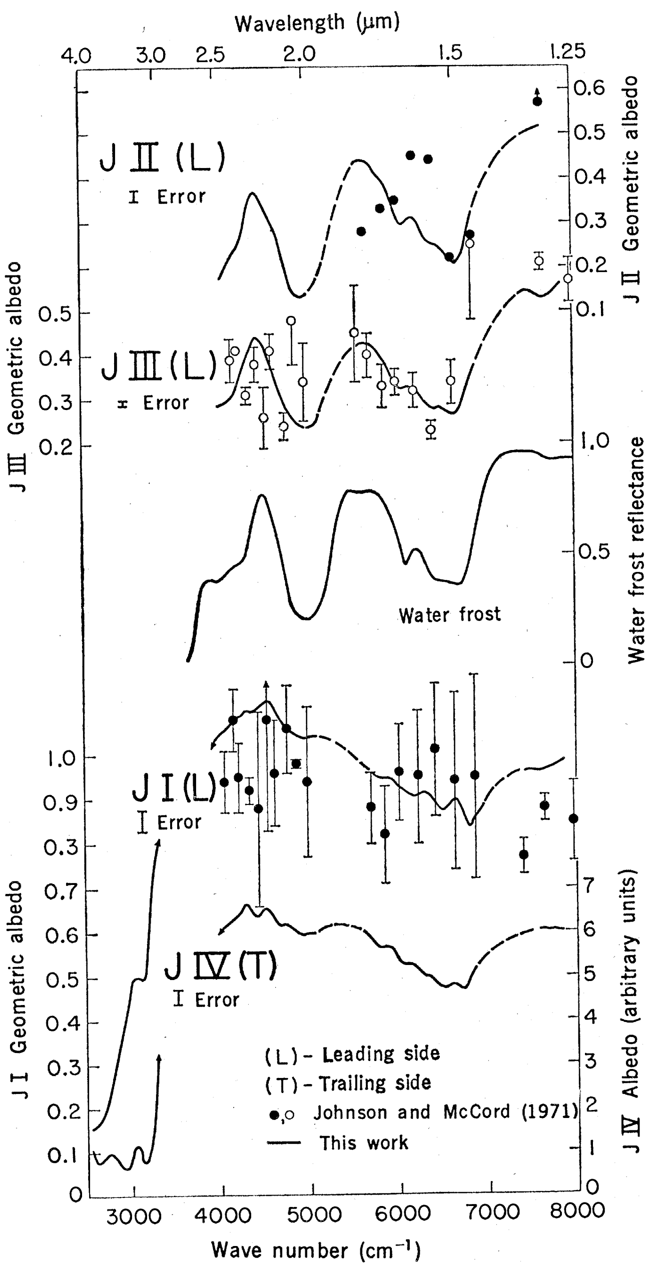

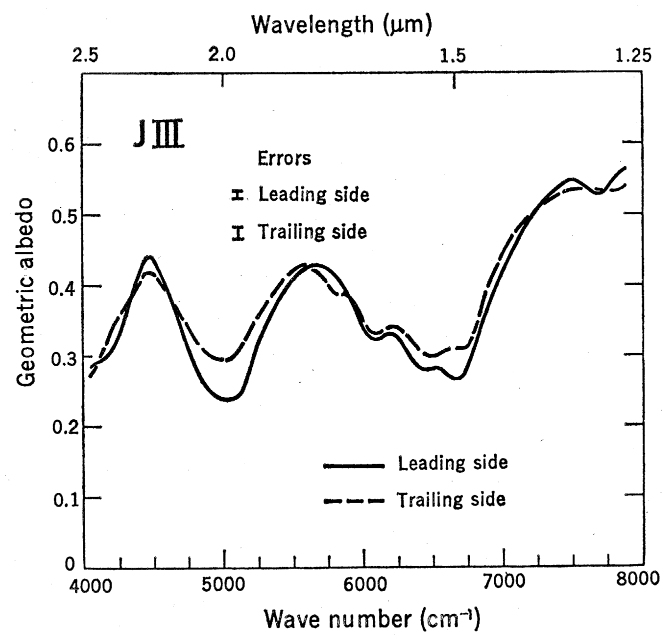

Fig. 1 (left). Reflectivities of the Galilean satellites and water frost. The reflectivities of JI, JII, and JIII have been scaled approximately to the geometric albedos of Johnson and McCord (*10*). Each error bar is the average of the standard deviations for all wavelengths. The intensities of the reflectivities of JI and JIV between 2500 and 3300 cm^{-1} are reduced below their proper values (see text). The water frost spectrum was measured at 77°K; its reflectance scale is relative to an MgO standard. Fig. 2 (above). The reflectivities of the leading and trailing sides of JIII scaled to the same value at 5625 cm^{-1}. Both reflectivities are also scaled to the geometric albedos of Johnson and McCord (*10*). Each error bar is the average of the standard deviations for all wavelengths.

contrary to the trend shown by the geometric albedos of JII, JIII, and JIV. The satellite reflectivities are consistent only with a process that links decreasing absorption intensity to decreasing albedo. Another such process, geometrically analogous to the one described above, is the mixing of dark, nonfrost materials with the frost on the satellites' surfaces.

We note that as we move out in the satellite system from JII, not only do the absorption intensities decrease, the overall slopes of the satellite reflectivities change from albedo decreasing to albedo increasing with wavelength. This is consistent with a partial surface cover model in which the underlying material is a silicate, since almost all silicates show albedos increasing with wavelength (*21, 23*).

Satellite JI has anomalous characteristics that do not allow it to fit readily into the above discussion. Its infrared spectrum resembles that of JIV, but it is almost three times more reflective than JIV in the visible. The high visible reflectivity of JI suggests that it is extensively frost covered, but the absence of strong absorptions in its infrared reflectivity indicates that, if frost is present, the particles are much smaller than those on JII and JIII. Small frost particles might be produced from the disruption of larger particles by electrons from the high flux around JI (*25*). Charged particle radiation acting on impurities, such as sulfides, in a frost on JI might also explain its ultraviolet-visible absorption (*22, 24*). Laboratory measurements of the reflectivities of pure and impure frosts struck by charged particles would be useful in examining such a model.

Veverka (*26*) also suggested that charged particle radiation has altered the infrared reflecting characteristics of JI. He concluded from polarization measurements that snow predominates on the surfaces of JI, JII, and JIII, and rock predominates on the surface of JIV; this is consistent with our conclusions for JII, JIII, and JIV, based on their infrared reflectivities.

Figure 2 shows the infrared reflectivities of the leading and trailing sides of JIII, scaled to the same value at 5625 cm^{-1}. The water frost absorptions on the leading side are deeper, the intensity difference indicating a 20 percent greater frost cover. This is in good quantitative agreement with the observed 15 percent brightness difference between the two sides (*15, 22*). Since the leading and trailing sides of JII differ in brightness by 30 percent (*15, 22*), JII may show a greater absorption intensity difference between its two sides than JIII. A single observation of the trailing side of JI, not presented here, shows a stronger increase in reflectivity with wavelength than on the leading side and a maximum near 5000 cm^{-1}. More data for both sides should be obtained for all the satellites.

CARL B. PILCHER

Department of Chemistry and
Planetary Astronomy Laboratory,
Department of Earth and Planetary Sciences, Massachusetts Institute of Technology, Cambridge 02139

STEPHEN T. RIDGWAY

Kitt Peak National Observatory,
Tucson, Arizona 85717, and
Department of Physics,
State University of New York,
Stony Brook 11790

THOMAS B. MCCORD

Planetary Astronomy Laboratory,
Massachusetts Institute of Technology

References and Notes

1. G. P. Kuiper, in *Atmospheres of the Earth and Planets* (Univ. of Chicago Press, Chicago, ed. 2, 1952), p. 340.
2. T. B. McCord, T. V. Johnson, J. H. Elias, *Astrophys. J.* **165**, 413 (1971).
3. C. B. Pilcher, C. R. Chapman, L. A. Lebofsky, H. H. Kieffer, *Science* **167**, 1372 (1970).
4. G. P. Kuiper, D. P. Cruikshank, U. Fink, *Sky Telesc.* **39**, 14 (1970).
5. G. P. Kuiper, in *Planets and Satellites*, G. P. Kuiper and B. M. Middlehurst, Eds. (Univ. of Chicago Press, Chicago, 1961), vol. 3, p. 305.
6. V. I. Moroz, *Sov. Astron. AJ* **9**, 999 (1966).
7. H. Kieffer, *J. Geophys. Res.* **75**, 501 (1970); thesis, California Institute of Technology (1968).
8. ———, personal communication.
9. L. Gromova, V. I. Moroz, D. P. Cruikshank, *Astron. Circ.* **569**, 6 (1970).
10. T. V. Johnson and T. B. McCord, *Astrophys. J.* **169**, 589 (1971).
11. D. Morrison and D. P. Cruikshank, in preparation.
12. J. S. Lewis, *Icarus* **15**, 174 (1971).
13. H. L. Johnson, I. Coleman, R. I. Mitchell, D. L. Steinmetz, *Commun. Lunar Planet. Lab.* **7**, 83 (1968).
14. T. B. McCord and T. V. Johnson, *Science* **169**, 855 (1970).
15. D. L. Harris, in *Planets and Satellites*, G. P. Kuiper and B. M. Middlehurst, Eds. (Univ. of Chicago Press, Chicago, 1961), pp. 291–293.
16. J. Stebbins and T. S. Jacobsen, *Lick Obs. Bull. No. 401* (1928).
17. B. T. O'Leary, paper presented at the 4th annual meeting of the Division of Planetary Sciences of the American Astronomical Society, Kona, Hawaii, March 1972.
18. P. Fellgett, thesis, University of Cambridge (1951).
19. G. P. Kuiper, D. P. Cruikshank, U. Fink, *Bull. Amer. Astron. Soc.* **2**, 235 (1970).
20. F. C. Gillett, K. M. Merrill, W. A. Stein, *Astrophys. Lett.* **6**, 247 (1970).
21. J. A. Adams and A. L. Filice, *J. Geophys. Res.* **72**, 5705 (1967).
22. T. V. Johnson, *Icarus* **14**, 94 (1971); thesis, California Institute of Technology (1969).
23. G. R. Hunt and J. W. Salisbury, *Mod. Geol.* **1**, 283 (1970).
24. T. V. Johnson and T. B. McCord, *Icarus* **13**, 37 (1970).

P. Goldreich and D. Lynden-Bell, *Astrophys. J.* **156**, 59 (1969).

J. F. Veverka, *Icarus* **14**, 355 (1971).

27. One of us (C.B.P.) was a visiting astronomer at Kitt Peak National Observatory. The observatory is operated by the Association of Universities for Research in Astronomy for the National Science Foundation. We thank H. Kieffer for allowing us to use his water frost spectrum prior to its publication as well as for many helpful discussions. C. Chapman reviewed the manuscript and made many useful suggestions. Helpful discussions were also held with T. Johnson and C. Reisz. The Idealab Fourier spectrometer was made available to us by the Astronomy Program of the State University of New York, Stony Brook. This work was supported in part by an NSF grant to the State University of New York, Stony Brook, and NASA grant NGR 22-009-473. Contribution No. 64 from the Planetary Astronomy Laboratory, Department of Earth and Planetary Sciences, Massachusetts Institute of Technology. Send correspondence to C.B.P.

15 September 1972

Internal Gravity Wave–Atmospheric Wind Interaction: A Cause of Clear Air Turbulence

Abstract. *The interaction between an internal gravity wave and a vertical wind shear may be responsible for the production of clear air turbulence in the free atmosphere. A simplified model equation demonstrates the feasibility of the suggested mechanism.*

Clear air turbulence (CAT) consists of all turbulent motions in regions of the free atmosphere that are not close to visible convective activity. It not only menaces aviation, but is also important in atmospheric circulation. A review of scant observations of CAT (*1*) shows that it appears in sporadic patches of apparently stable atmospheric layers with vertical wind shear. When CAT occurs, spectral analyses of the atmospheric motions consistently exhibit a marked gap in the spectral energy density, $E(k)$ (*2*). The "spectral gap" is accompanied by an energy bulge at higher wave numbers. Various hypotheses have been advanced to explain the occurrence of CAT associated with this spectral energy bulge (*1*). It is often speculated that the most likely energy source for CAT is the shear present in large-scale wind structure,